

Investigation of Natural Mucilage for Enhanced Oil Recovery: the Potential of *Corchorus Olitorius* Hydrocolloid

Azza Hashim Abbas,* Ghalymzhan Serikov, Yermukhan Zhuniskenov, Neda Eghtesadi, Kamel Fahmi Bou-Hamdan, and Tri Thanh Pham*



Cite This: *ACS Omega* 2023, 8, 29693–29703



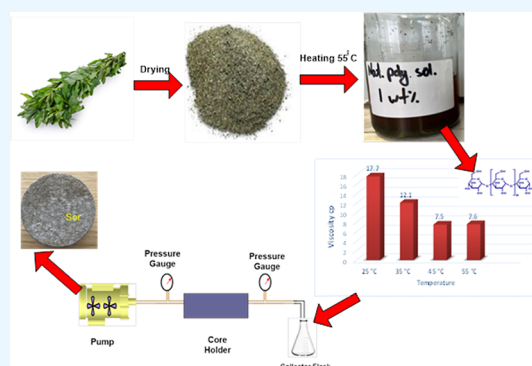
Read Online

ACCESS |

Metrics & More

Article Recommendations

ABSTRACT: The need for an effective offshore enhanced oil recovery (EOR) solution led to the focus on natural hydrocolloids. Polysaccharide hydrocolloid research is constantly expanding in a variety of petroleum applications such as drilling, flow assurance, and EOR. *Corchorus olitorius* is being examined in the present study as a potential natural polymer for chemical flooding. This study investigated the rheology and fluid flow characteristics in porous media, focusing on the effects of the concentration, temperature, and salinity of the fluid. Furthermore, core flooding was carried out to evaluate the potential recovery was characterized and found to contain a significant amount of polysaccharides and cellulose. The rheological behavior demonstrated an increase in viscosity with concentration. The relationship between viscosity and temperature is inversely proportional. Additionally, the mucilage viscosity significantly increased in the presence of 35,000 ppm NaCl, varying from 39 to 48 cp. The improvement of oil recovery by a unit PV injection is around 10 and 20% at 0 and 35,000 ppm of NaCl, respectively. In sandstone with a moderate porosity and permeability, the overall oil recovery ranges between 59 and 70%. *C. olitorius* has complex polysaccharide/cellulose derivatives that improved rheology and produced results that are promising for future offshore applications.



1. INTRODUCTION

Current endeavor in the enhanced oil recovery (EOR) research is to identify alternatives to the conventional EOR method. The philosophy emphasizes enhancement, customization, and optimization. For instance, cutting back on the amount of chemicals or gases used in the process is because the first is very expensive and the second has technical management issues, which raises the project cost.^{1,2} The second attempt has been made to assess the effectiveness of these materials. The material may be adequate for a period of time before degrading or reacting with the formation, making it impractical to continue operating effectively. Due to environmental concerns, reducing the discharge of offshore chemicals became critical and many regulations and rules were constantly updated.³ As a result, the development of new environmentally friendly workable chemicals is necessary.^{1,4,5}

Successful chemical applications rely on the tentative improvement of microscopic and macroscopic sweep in various geological configurations. Polymers, surfactants, alkalis, and polymeric surfactants are the primary injectants as solutes.⁶ Several technical, economical, and environmental factors influence the extent to which these chemical EOR (CEOR) methods are used.^{4,7} Technically, the chemical used should be capable of minimizing the mobility ratio or

interfacial tension under reservoir conditions. At the reservoir scale, the effect of geological type, pH, salinity, temperature, and pressure on the performance of the chemical technique is critical.⁸

There are numerous problems associated with excessive chemical use. The chemicals applied are mainly petroleum-based. Because oil fields are massive in size, the quantities of chemicals required are enormous and costly as well. The goal of sustainability and development necessitates strict environmental control. As a result, environmental regulations must be implemented in industrial operations. Chemical assessment of the impact of near freshwater formation is required in chemical practice. Furthermore, the chemicals chosen must be nontoxic and easily separated from the oil.

Polymers are among the most extensively used chemicals in large oil fields.⁹ Polymer flooding is a procedure in which polymers are introduced to the water of a waterflood to reduce

Received: May 31, 2023

Accepted: July 19, 2023

Published: July 31, 2023





Figure 1. Preparation of *Corchorus olitorius* mucilage solution.

its mobility. This is accomplished by increasing viscosity and thereby decreasing aqueous phase permeability. Polymer does not mix with oil. Thus, the oil permeability remains unaltered. The reduction in water permeability is the primary cause of the lower mobility ratio. Any mobility ratio less than one is considered favorable. As a result, a reduced mobility ratio improves the waterflood efficiency by improving volumetric sweep efficiency. Despite previously established facts, polymer solution can modify the flow path. This is due to the crucial flow term (resistant factor), which refers to the resistance to flow encountered by a polymer solution in comparison to plain water flow. To truly comprehend polymer flooding, however, one must first understand the complicated rheology, which includes shear thinning/thickening, thermal stability, biodegradation, reservoir pH, and salinity tolerance and injectivity.

The search for suitable polymers resulted in the acceptance of hydrocolloids from natural sources to be used.¹⁰ Hydrocolloid polymers can be derived from plants, microbial or chemical modification of natural polysaccharides.¹¹ The common denominator is that they have multiple hydroxyl groups and may be polyelectrolytes. These hydrocolloid natural polymers often have long polysaccharide chains, which is useful for withstanding harsh reservoir conditions. Xanthan gum is a leading polymer for such applications. Xanthan gum is extremely viscous in solution and can withstand a wide range of environmental conditions, including pH, ionic strength, heat, and enzymes.¹² Although natural polymers are more prevalent in CEOR, they are highly demanded in other sectors. For example, a naturally cross-linked polymer is used as a diverting agent in fracture reservoirs.¹³ In general, the demand for polysaccharide hydrocolloids is rising rapidly across a range of petroleum applications. When looking at polysaccharide examples, a range of natural polymers were discovered, including guar gum, flaxseed gum, welan gum, and okra, among many others. According to Gao, welan gum recovered 72% of the original oil in place and reduced the time required to achieve residual oil saturation.¹⁴ Polymer flooding based on guar gum has been shown to recover up to 16% of the original oil in place at the secondary recovery stage.¹⁵ The incremental oil recovery from okra flooding in carbonate was 7%, which was supported by mechanical trapping of the big molecule size in the low porosity–permeability core.^{16,17} According to our observations, the recovery factor varies widely. Such variance could be justified by the type of oil, tested cores, polysaccharide quantity, and viscosity.

Corchorus olitorius is a green plant of the Tiliaceae family. The leaves are edible throughout most of the Mediterranean and North Africa, where there is a rich culinary history. In Arab countries, the plant is known as molokhia, while in South Asian countries, it is known as jute. The plant contains minerals like

calcium, magnesium, and dietary fiber.¹⁸ Thus, the leaves of *C. olitorius* are an excellent source of hydrocolloids.¹⁹ The main attraction is the presence of water-soluble mucilage.²⁰ It was observed that the viscosity of *C. olitorius* leaves suspended in distilled water has dramatically increased. Additionally, it was challenging to remove the polysaccharide without additional processing. EI-Mahdy and EI-Sebaiy (1984) investigated mucilage and discovered that fresh leaves had a lower viscosity than the predicted polysaccharide.²¹ The link between the polysaccharide structure and function is unknown because it is dependent on molecular weight, monosaccharide composition, and polysaccharide biological activity.²² Despite the difficulties in characterizing the polysaccharides previously, the primary concern is the increased viscosity favorable for mobility ratio alteration. *C. olitorius* biproduct/waste has recently been utilized to treat the corrosion of oil and gas pipes.²³

To summarize the findings, it is worth noting that there has been relatively little effort devoted to examining polysaccharides. *C. olitorius* has not been studied for EOR applications in the oil and gas industries. Therefore, the main challenge is defining the range that will make the material effective for field practice. As a result, it is necessary to address and comprehend its rheology and fluid flow properties in porous media. Thus, this study has two goals: (1) to assess the impact of its concentration, temperature, and seawater salinity and (2) to validate the implementation in core flooding conditions on a laboratory scale.

2. METHODOLOGY

2.1. Material Preparation. *C. olitorius* leaves (2 kg) were purchased from the local market in Khartoum, Sudan. The leaves were washed with distilled water three times. The leaves were left to dry under the sun, as shown in Figure 1. The dried leaves were collected and crushed into powder form. The crushed powder was then sieved by a strainer of 3.38". The mucilage in the *C. olitorius* leaves was prepared for three main concentrations of 1, 2.5, and 5 wt % by putting the powder in deionized water (DIW) at a temperature of 50 °C and continuously stirring at 100 rpm for 20 min. The liquid formed was then filtered using a filter cloth.

2.2. Material Characterization. **2.2.1. Group Function Characterization.** Fourier-transform infrared spectroscopy (FT-IR) was used to characterize the group function. This type of examination is known as FT-IR analysis or FT-IR spectroscopy, and it is used to detect organic, polymeric, and in some cases, inorganic materials. FT-IR was used to characterize the functional chemical groups and structures of the *C. olitorius* samples. FT-IR spectra were gathered using the Nicolet iS10 FT-IR spectrometer equipped with a ZnSe flat crystal. OMNIC software was used to collect the graphs. The background spectrum was collected initially and compared

with the reference background spectra for each sample. The smashed and powdered samples (20 mg) were then applied to the crystal, and the pressure was adjusted. Spectra were determined by recording 32 transmission scans in the range of 4000–400 cm^{-1} with a resolution of 4 cm^{-1} . The ratio between the sample and background spectrum displays the sample spectrum.

2.2.2. Surface Morphology. A JEOL JSM-IT200 (Tokyo, Japan) device of electron microscopy was used to visualize the morphology and chemical components of the samples. Turbomolecular Pumped Coater Q150T (Quorum Technologies, UK) was used to coat the sample before the scanning electron microscopy (SEM) analyses. Different magnifications were used to identify the morphology details. Additionally, combined with SEM, the microscale chemical composition of the samples was analyzed in the area of 10 μm using energy-dispersive X-ray spectroscopy.

2.3. Rheology. The viscosity of the green chemical solution was measured using a Physica Modular Compact Rheometer 302 from Anton Paar. Since the green chemical was used in low concentrations, it was considered a low-viscosity fluid and a volumetric measuring cylinder was used. The experiment was conducted following all technical safety rules to ensure accurate results. Approximately 50 mL of each concentration was used to fill the measuring cylinder. The apparatus was turned on for an hour before measurement, and the temperature was set for 20 min until the solution reached the desired temperature. The shear rate was set to a range of 1–1000 1/s before the measurement. The temperature examined range was at 25, 35, 45, and 55 $^{\circ}\text{C}$.

The results were modeled mathematically by Ostwald–de Waele, as shown in eq 1

$$\eta = K\dot{\gamma}^{n-1} \quad (1)$$

n is the flow behavior index, K is the flow consistency index, $\dot{\gamma}$ is the shear rate, and η is the apparent viscosity. n value explains the degree of nonlinear behavior. According to Ostwald's power law, the viscosity of a substance varies as a function of shear rate. When the exponent " n " in the equation is less than one, the viscosity decreases as the shear rate increases; this is known as shear thinning or pseudoplastic behavior. When the value of " n " is greater than one, the viscosity rises as the shear rate increases, a phenomenon known as shear thickening or dilatant. When " n " is exactly one, the viscosity remains constant regardless of the shear rate.²⁴ The study was conducted using a reservoir temperature of 55 $^{\circ}\text{C}$, which reflects the conditions of the potential field being studied.

2.4. Core Flooding Experiment. The core flooding and core characterization were done using Vinci Technologies France's ACA-700 Aging cell apparatus. Berea sandstone samples were obtained from Kocurek, USA. Porosity was examined by a Porosimeter device from Vinci Technologies France, as shown in Figure 2c. Afterward, the porosity was calculated by obtaining the difference between the dry and wet weights of the core, as shown in Table 1. Next, the permeability of the cores was calculated using pressure difference values while injecting DIW at different rates from 0.5 to 5 mL/min. Calculations were performed using Darcy's equation. The procedure standard was followed, as stated earlier in ref 25. For saturation, first, the clean core was flooded with DIW until the water was produced. Following this step, the core was left in the DIW water bath for 24 h before further

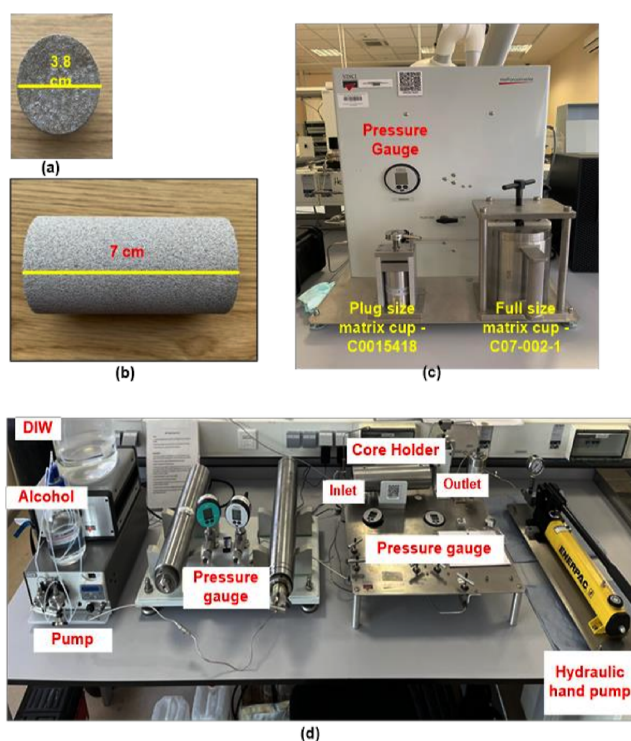


Figure 2. Photo of the equipment used. (a,b) Core dimensions, (c) porosimetry, and (d) core flooding setup.

use to ensure wettability preservation. Afterward, the flooding of synthetic oil decane (a density of 725.5 kg/m^3 and a viscosity of 0.838 $\text{mPa}\cdot\text{s}$) was used. The core was placed under a confining pressure of 1100 psi and was used to create an overburden on the rock sample. The back pressure was set to 500 psi. The oil was injected up to 5 PV of oil injected. The injection was stopped when there was no additional water was produced. Noting that when the first oil pore volume was fully produced, the initial water saturation was calculated.

The main experiment steps for both mucilages were typical. The saturated core was flooded with 5 PV of DIW or brine until no oil was produced. Following this, 1 PV of 5 wt % of *C. olitorius* leaves solution was injected as the primary flush at ambient temperature. For the post flush, only pure water was produced after 5 PV of DIW/brine being injected.

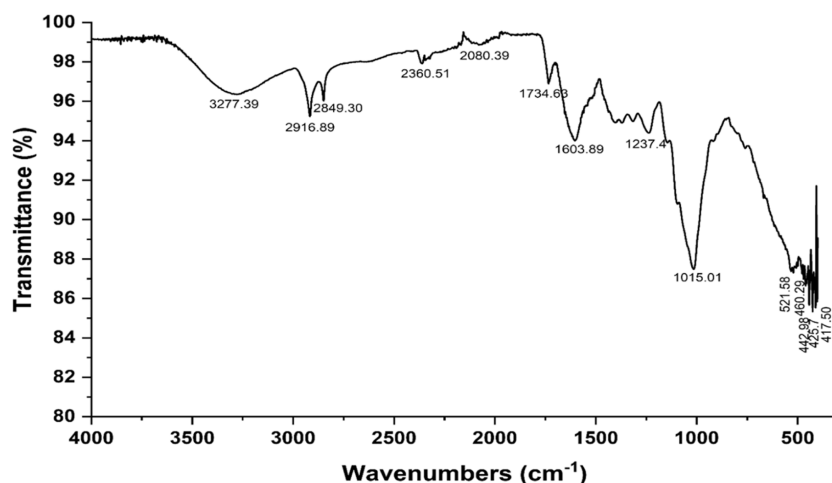
3. RESULTS AND DISCUSSION

3.1. Corchorus olitorius Characterization. Figure 3 shows various peaks observed between 4000 and 400 cm^{-1} . The first observed peak is at 3277 cm^{-1} , which occurs due to the hydroxyl (OH) stretching vibration, mainly related to phenolic compounds. The peak that appeared in 2916 cm^{-1} is attributed to cellulose, hemicellulose, and lignin. It represents the typical C–H.²⁶ The region between 2080 and 2849 cm^{-1} corresponds to organic esters, including fatty acid methyl esters and phenolic acid methyl esters. These peaks exhibit variations in intensity depending on the level of increase in the water content. The peak at 1734 cm^{-1} refers to C=O stretching of the ester linkage in hemicelluloses.²⁷ The peak situated within region 1610–1619 cm^{-1} is reflecting the C=C. A similar observation was reported in ref 28.

The peak of 1401 cm^{-1} , which denotes hemicellulose, provides further proof of the cellulose content. On the other hand, the broad peak of 1237 cm^{-1} is ascribed to the methoxyl

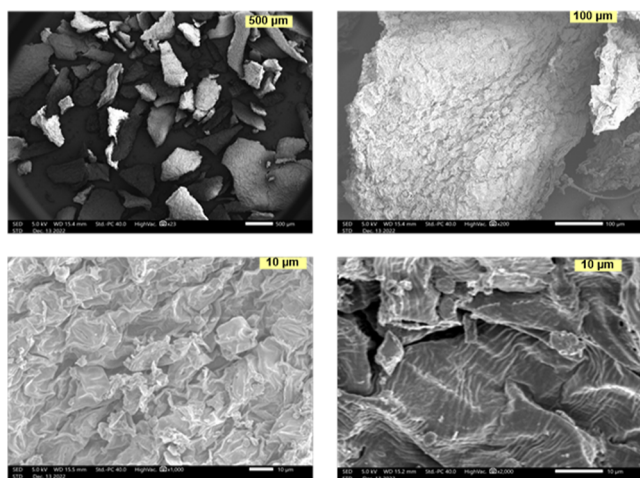
Table 1. Core Properties

core ID	length (cm)	diameter (cm)	PV (cm ³)	bulk volume (cm ³)	porosity (%)	S _{wi} (%)	permeability (mD)
Berea sandstone 1	7	3.8	16.9	80.96	20.87	33.3	230
Berea sandstone 2	6.4	3.8	15.45	72.64	21.27	32.3	235

Figure 3. FTIR data for *Corchorus olitorius*.

groups from the lignin structure. Yet, when the results are analyzed regionally, the polysaccharide is verified by the peaks in the range of 1000 and 1237 cm⁻¹. The steep peaks in the area indicate the stretching vibrations of CO and OH. This most commonly refers to the polysaccharide found in cellulose. It is worth noting that the phenol compounds are high due to the leaves drying process by the sun, as stated earlier in ref 29. The band at 1015 cm⁻¹ indicates D-glucose.

The surface morphology presented in Figure 4 shows that the sample is sheet-like. There is no specific format that can be

Figure 4. SEM images of *Corchorus olitorius*.

assigned. However, the edges are semi-rounded with no sharpness. The size is approximately between 100 and 800 μm. The SEM output at a magnification of 200 times shows a smooth surface with no pores. Furthermore, both magnification of 1000 and 2000 confirms the closely packed sheet and the amorphous no porous morphology nature. The mechanical and dimensional stability at high temperatures can be obtained at any dense morphology with no observed porous. A similar

observation of *C. olitorius* powder particles was observed in ref 30.

Elemental analysis, as shown in Figure 5, confirms a high carbon (C) content and limited oxygen (O). This verifies the nature of complex cellulose and polysaccharides. It also indicates the presence of C=O. More ions seem to be available with low content, such as Mg, Ca, and K. The low mineral components are additional evidence of the constitute of *C. olitorius*. The EDX screening justifies the difference between typical cellulose and polysaccharide compared to *C. olitorius* raw nature.

3.2. Effect of Concentration on Rheology. Up to a certain point, the increase in the hydrocolloid concentration increases the viscosity. Despite the general consensus that polymer concentrations must be as high as possible to be effective, subsurface flooding experiments demonstrate that pores can become clogged. The previous literature screening criteria revealed that 5000 ppm of synthetic polymer is the technical limit.³¹ A previous study also reported that biopolymer implementation could be successful at as low as 800 ppm,³² which is significantly lower than what has been reported for natural polymers.^{17,33}

As seen in Figure 6, the trend of viscosity rapidly increased by 10 times compared to water viscosity at the lowest concentration of 1 wt %. As the viscosity change is proportional to the number of molecules present, further concentration increase to 2.5 and 5 wt % results in 20- and 50-times larger viscosity values than water, respectively.

The highest viscosity observed is at 5 wt %. This is explained by additional large polysaccharide molecules, which increases drag and interacting forces. A previous description of the effect of low shear rate on various polysaccharides (shear rate from 1 to 100 s⁻¹) unveiled direct link between contiguous polymer chains or structural breakdown and the rapid shear thinning.¹¹

From the results of rheology testing, polymer viscosity values depend on shear rates. The polymer has maximum viscosity values at the lowest possible shear rates. This trend is observed for all three concentrations. Moreover, with the same viscosity

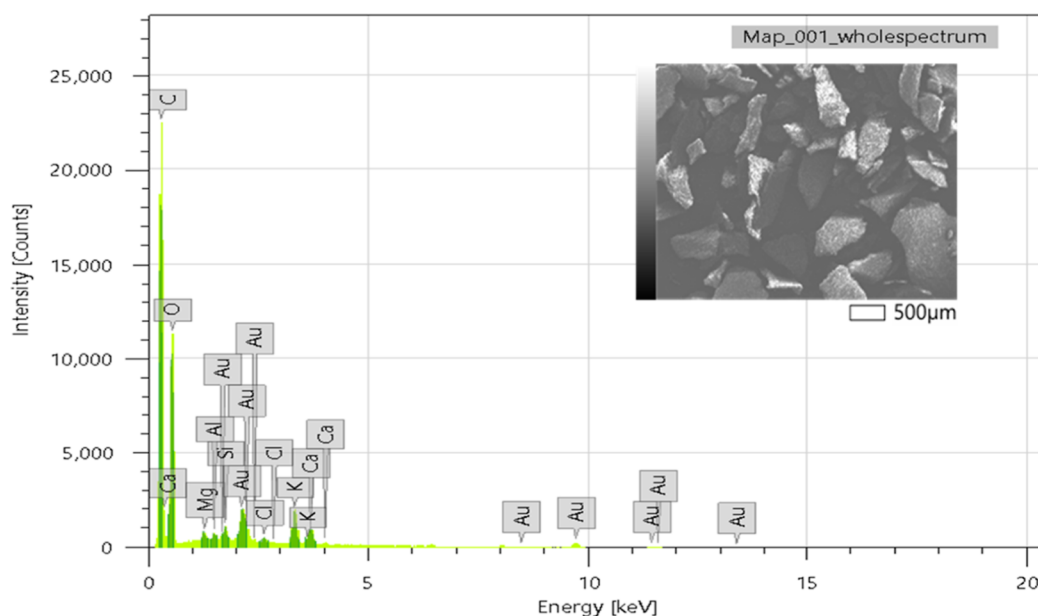


Figure 5. Elemental analysis of *Corchorus olitorius*.

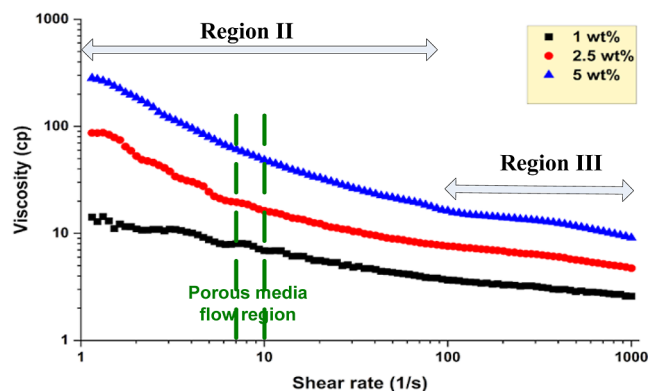


Figure 6. Effect of *Corchorus olitorius* concentration on viscosity under different shear rates.

profile, *C. olitorius* with a concentration of 5 wt % has viscosity values twice higher than a 2.5 wt % concentration for all given shear rate values. As the shear rate increases, hydrocolloid viscosity decreases, compared to intricately intertwined superstructures, individual molecules exhibit lower resistance to flow. This represents the shear-thinning behavior of the *C. olitorius* macromolecule solution.

Shear thinning polymers are usually the main interest in EOR application of polymer flooding. Their main distinctive characteristics are high viscosity values within low shear rates. The interest in shear rates between 7 and 10 s^{-1} terms from the fact that they correspond to the possible flow in porous media.^{17,34} Furthermore, the shear rate between 150 and 300 s^{-1} represents the expected shear rate in the vicinity of the well region.³⁵ It is clear from the previous polymeric solution investigations that the relationship between polymer viscosity and shear rates exhibits curves with three distinguished regions (I, II, and III). Region I corresponds to low shear rates and lower Newtonian behavior of polymer due to insufficient level of shear to be obstructed by entanglements. Within this region, polymer viscosity is not affected by the shear rate. As Region I is only present at very low shear rates, it is not observed in Figure 6. This observation is related to the fact that it is not

under investigation for normal shear under hydrocarbon reservoir conditions.

Region II arises as a result of the stretching of molecules and their inclination to disturb the interconnected structure of the solution, which accordingly reduces the viscosity. Viscosity change versus shear rate is characterized by the Ostwald–de Waele model, which is further used to describe the behavior. From Figure 6, viscosity values for 1, 2.5, and 5 wt % are 7, 16, and 48 cp, respectively. The shear thinning region is observed for shear rate values between 10 and 100 1/s. Region III corresponds to the highest shear rate values and upper Newtonian behavior. Viscosity is not affected by shear rate increase as *C. olitorius* solution molecules break and lose viscosifying properties. Region III entrance or transition is noticed at shear rate values higher than 100 1/s. *C. olitorius* solution experienced no viscosity reduction entering Region III. Lately, a study of the effect of low shear rate on different polysaccharides from different sources confirmed the impact of polymer interaction and the structural alteration to the shear thinning mechanism.¹¹ This study endorses the region identified by the current study.

3.3. Effect of Temperature. The viscosity was measured under different elevated temperatures, the selected range including a reservoir temperature of 55 °C that represent Kazakhstan condition. Figure 7 shows the effect of temperature on different concentrations (1, 2.5, and 5 wt %) at different shear rates. Results show a decreasing trend of viscosity with an increase in temperature. A similar trend was observed for all three concentrations. Viscosity decrease was measured to be around 30–35% from initial values at 25 °C for every concentration.

This behavior is primarily attributed to the increased molecular mobility and reduced intermolecular forces within the natural polymer chains.^{10,36} Consequently, the viscosity of the polymer decreases as it becomes easier for the chains to slide past each other. The viscosity of polymer solutions with polysaccharides depends on various parameters such as molecule structure, concentration, and the presence of other substances. The trend of viscosity tends to increase at the

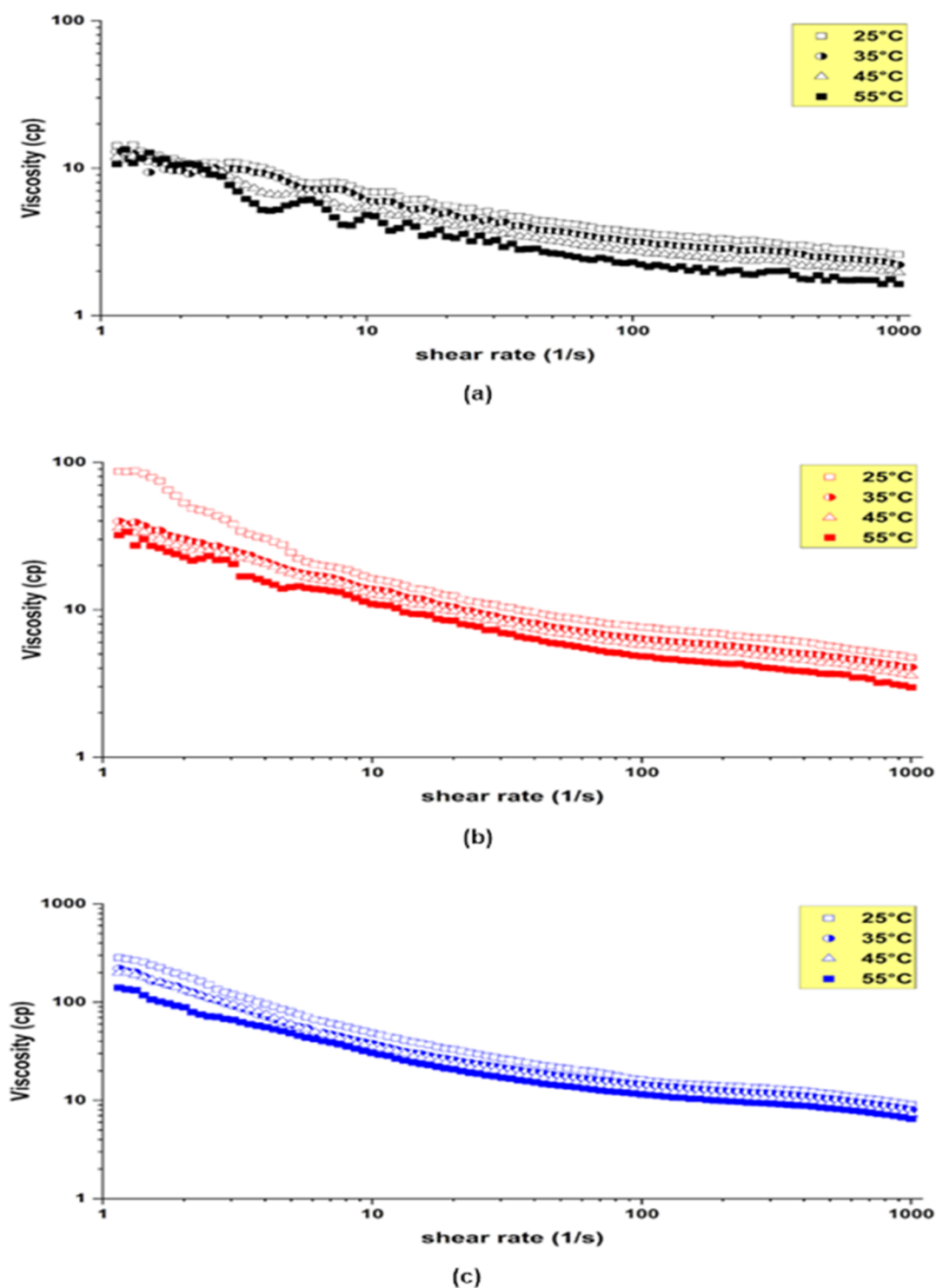


Figure 7. Effect of temperature on *Corchorus olitorius* viscosity under different shear rates (a) 1 wt % concentration, (b) 2.5 wt % concentration, and (c) 5 wt % concentration.

higher concentration of polysaccharides. Because intermolecular interactions become more frequent. Also, the greater the molecular weight of the polysaccharides, the greater the chain link, which results in higher viscosity. According to the research by Abbas et al., (2013), most polysaccharide polymers show a decreasing trend as the temperature increases and viscosity is greater in high-concentration polymers. Polymers used in this work have similar tendencies.³⁷ Also, other research on scleroglucan by Fortenberry et al., (2017), which

has a helix structure of repeating polysaccharides, showed a decreasing trend as shear increases.³⁸ The viscosity at 10 s shear was close to values in this research, and the viscosity reduction under higher temperatures was reported. Our observations indicate that the *C. olitorius* is effective under reservoir temperature. For example, from Figure 7, the *C. olitorius* 5 wt % solution results in 40 cp, while 2.5 and 1 wt % are lower around 18 and 4 cp. These values show that the

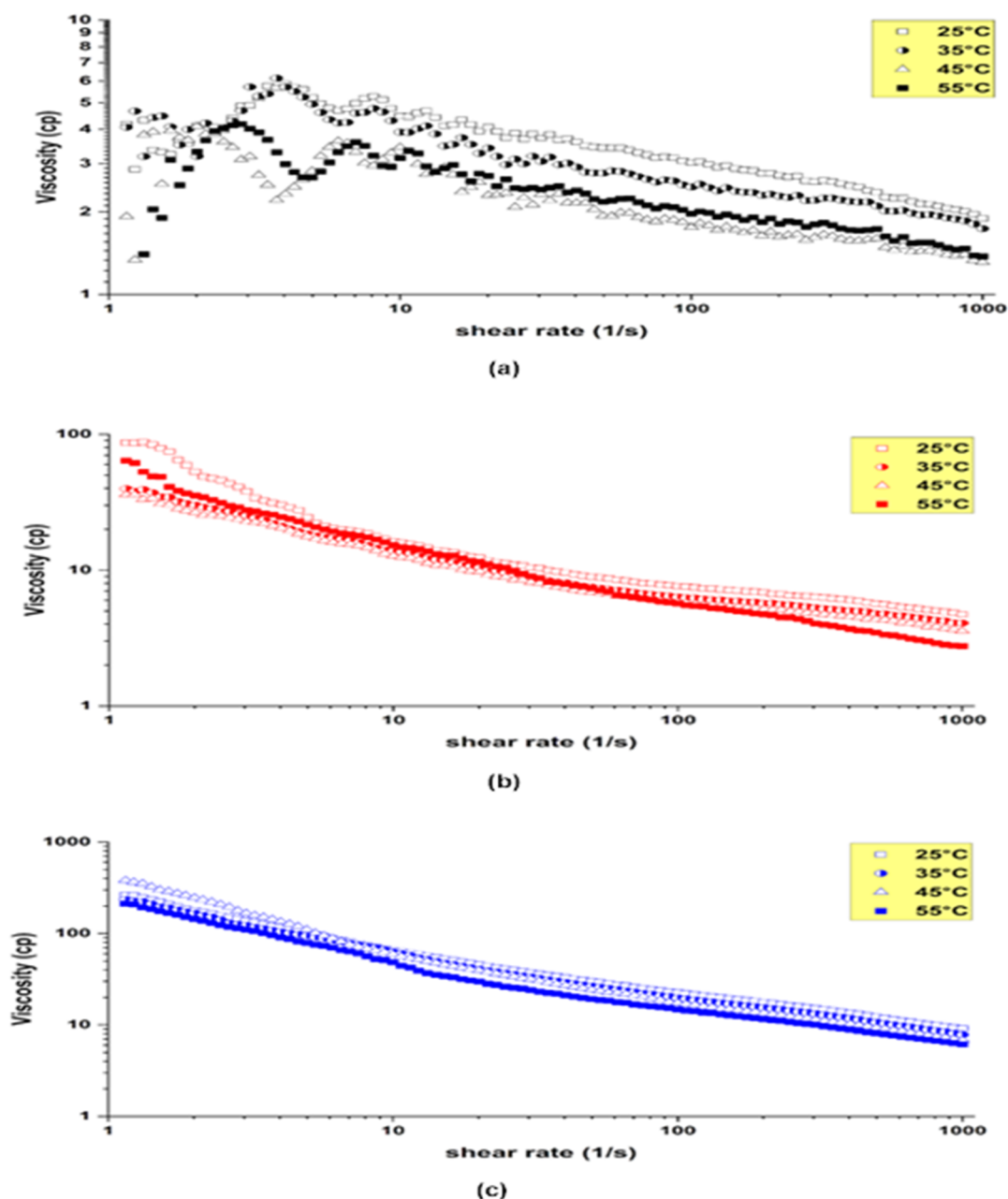


Figure 8. Effect of seawater salinity and temperature on *Corchorus olerius* viscosity under different shear rates (a) 1 wt % concentration, (b) 2.5 wt % concentration, and (c) 5 wt % concentration.

solution can even be used in higher temperatures for harsh condition.

3.4. Effect of Salinity under Reservoir Temperature.

In offshore practice, the tendency to apply chemicals is associated with seawater as the main source of solvent. Therefore, the effect of seawater represented by 35,000 ppm of NaCl along with temperature was studied. It is well known in the literature that polymers behave differently in the presence of salinity. Salinity is commonly identified as a cause of carbon chain breakdown. However, the salinity tolerance can be enhanced if the polymer's carbon numbers increased. When NaCl is introduced into polymers, the electrolyte's double layer defines the repulsive forces and the polymer chain expansion is reduced due to the ions. Divalent ions readily attract to any negative charge that the polymer carries. This makes the divalent ions a harsher condition than monovalent

ions.³⁹ However, in the case of natural polymers, this effect is noticeably weaker and nearly identical for both divalent and monovalent ions. In contrast, introducing monovalent cations can increase the polarity and result in denser chain-hydrophobic network. Regardless of the general explanation, it is critical to analyze performance and its effects on rheology.

Figure 8 shows the synergetic effect of seawater salinity and temperature on different concentrations (1, 2.5, and 5 wt %) at different shear rates. Results show increased viscosity values of *C. olerius* at seawater salinity. The increase in viscosity is more than that in the 0 salinity solutions. For instance, comparing polymer solutions of 35,000 ppm of NaCl with 0 salinity solution, a 15% increase in viscosity is observed. In the absence of NaCl and reservoir temperature, the viscosity reached 40 cp, while with a salinity of 35,000 ppm NaCl, it reached 48 cp.

Table 2. Shear Model Parameters

salinity	temperature °C	concentration wt %	consistency index (<i>k</i>)	flow behavior index (<i>n</i>)	stability index (<i>R</i> ²)	
0 NaCl	25	1	13.62	0.73	1	
		2.5	36.65	0.66	0.99	
		5	113.23	0.60	0.95	
	35	1	12.29	0.72	1	
		2.5	30.90	0.66	0.99	
		5	81.70	0.633	0.95	
	45	1	11.56	0.69	1	
		2.5	30.021	0.65	0.99	
		5	81.08	0.61	0.95	
	55	1	10.48	0.66	0.86	
		2.5	25.51	0.65	0.95	
		5	71.68	0.61	0.96	
	35,000 ppm NaCl	25	1	6.19	0.85	0.85
			2.5	53.36	0.61	0.99
			5	173.48	0.56	0.98
35		1	5.55	0.84	0.77	
		2.5	48.28	0.59	0.99	
		5	166.69	0.54	0.99	
45		1	4.0	0.84	0.99	
		2.5	39.63	0.64	1	
		5	179.02	0.50	0.98	
55		1	4.34	0.84	0.95	
		2.5	42.76	0.57	1	
		5	128.77	0.53	0.99	

Remarkably, this behavior is explained by the presence of additional Na⁺ ions, which affect the polymer's polarity. The positive impact on polymers results from increased hydrodynamic volume and molecular chain elongation. For some polysaccharide polymers, the salinity can break the hydrogen bonding and other interactions that hold polysaccharide chains together.

The positive behavior of polymer viscosity on salinity increase eliminates application problems in saline reservoirs. As the following temperature and salinity values are consistent with Kazakhstan field, *C. olitorius* could be considered as an efficient and temperature–salinity-resistant candidate for Kazakhstan fields.

3.5. Shear Thinning Model. The behavior of non-Newtonian fluids under shear rate is described by shear thinning and thickening polymer models. Unlike Newtonian fluids, whose viscosity is not a function of shear rate, the viscosity of non-Newtonian fluids is highly dependent on shear rate or stress applied. As seen in Figures 6–8, the relationship of *C. olitorius* is shear thinning. Generally, the mechanism behind shear thinning is the alignment and stretching of polymer chains in response to the applied shear stress. One of the widely used models to describe shear thinning behavior is the Ostwald–de Waele model. Table 2 shows the effect of concentration on the Ostwald–de Waele model parameters, such as the consistency index (*K*) and the flow behavior index (*n*). The overall trend shows a decrease in the flow behavior index with increasing *C. olitorius* concentration. This is explained by more frequent intermolecular interaction of polysaccharides resulting in hindered flow and a decrease in fluid's sensitivity to shear rate changes.

In contrast to consistency, index is constantly increasing with concentration due to the entanglement of the molecules. It is clearly seen that consistency and flow behavior indexes decrease as the temperature increase. This is explained by the

loss of rheological properties of polymers under increased temperature. This decrease indicates lower viscosity, a shift toward shear-thinning behavior, improved flowability, and potentially more Newtonian-like flow behavior in the polymer solution. The effect of salinity and temperature simultaneously. Comparing the results of estimated parameters at 35,000 ppm salinity with samples measured in the absence of salinity, it is observed that the flow behavior index increases and the consistency index decreases with increased salinity. This is a clear indication that the polymer's rheological properties have been improved and salinity positively affects the natural polymer behavior. As ion concentration increases with salinity, the likelihood of ion–polymer interactions increases, causing an alteration of the polymer's rheological behavior and an increase in the flow behavior index.

3.6. Core Flooding. To create an effective chemical to regulate water mobility, water fingering, and front pattern in porous medium, the formed solution must be stable under reservoir conditions. As a result, investigating the flow behavior of dynamic flooding using core scale size is essential.⁴⁰

Berea sandstone cores used were characterized as moderate porosity–permeability with values of 21% and 230 mD, respectively. Figure 9a,b shows the oil recovery after injection of 5 wt % *C. olitorius* leaves solution with DIW and seawater brine with saline water. The injection result in the absence of salinity demonstrated an additional 15% of oil recovered after *C. olitorius* solution. On the other hand, the saline condition showed 20% of additional oil recovered. Both samples showed maximum recovery after 1 PV of polymer main flush followed by an additional 5–10% recovery after post flush. The results, as indicated in Table 3, show that applying *C. olitorius* leaves solution at higher salinities is more effective. This can be directly attributed to the viscosity enhancement. *C. olitorius* has better rheology in saline conditions with 15% viscosity enhancement.

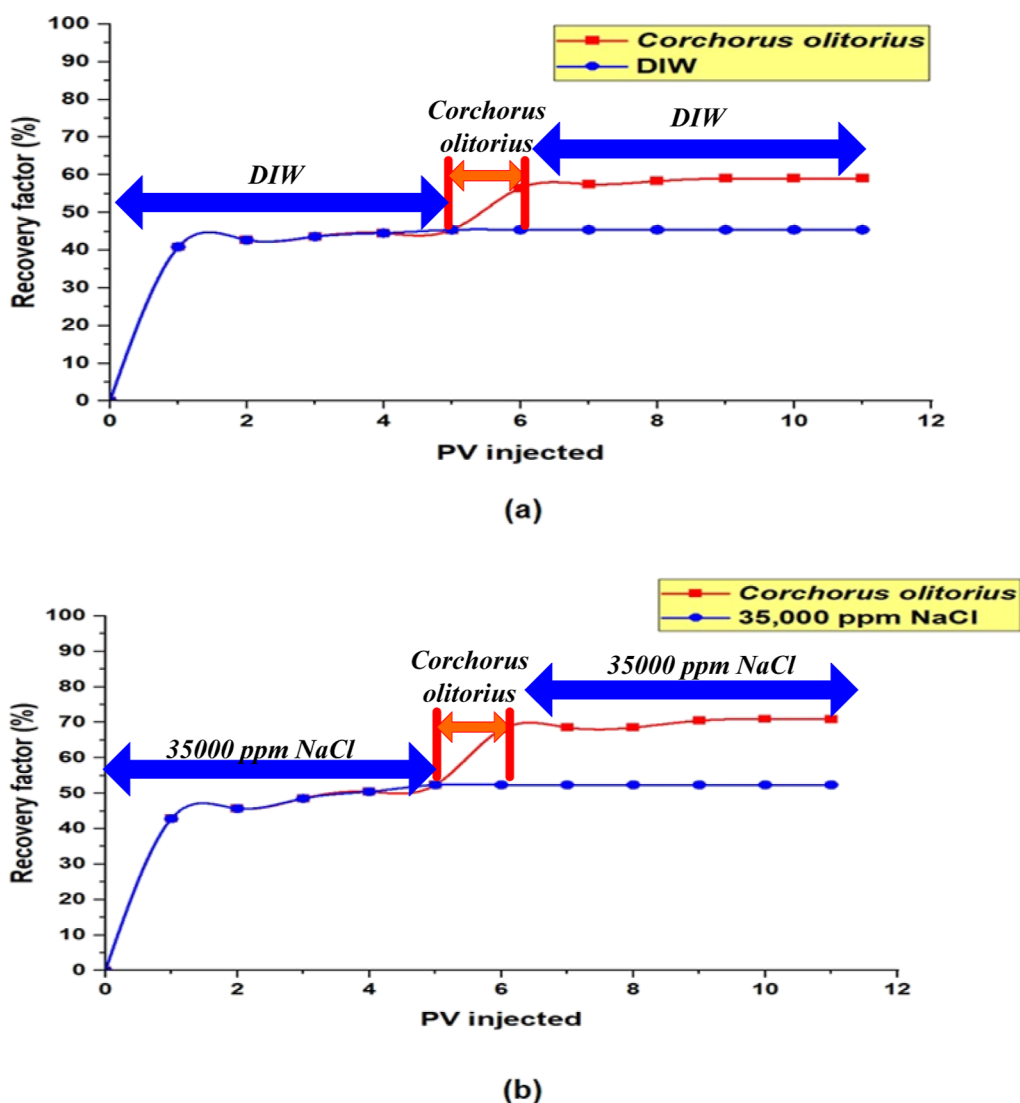


Figure 9. Core flooding (a) the implementation in 0 ppm salinity and (b) the implementation in 35,000 ppm.

Table 3. Core Flooding

parameters	core 1	core 2
<i>Corchorus olitorius</i> viscosity at 25C (cp)	48.5	65.5
<i>Corchorus olitorius</i> concentration (wt %)	5	5
salinity (ppm)	0	35,000
permeability to oil (mD)	127	135
water breakthrough after (PV injected)	1.5	1.5
% of OOIP from 5 PV of water	45%	52%
added % of OOIP after 1 PV of polymer	10%	15%
final % of OOIP after 5 PV of water	59%	71%
final oil saturation	27%	19%
estimated water saturation	33%	32%

C. olitorius solution was compared with alternative biopolymers used for EOR in Berea sandstones. Results showed that the application of *C. olitorius* as a viscosifying agent is as effective as Schizophyllan, Xanthan gum, and guar gum. According to Joshi et al. (2016), injection of 6 PV of Schizophyllan biopolymer results in an additional 28% of oil recovered with an initial water flooding recovery of 51%. These results could be compared with 20% of additional oil recovery

after 1 PV of *C. olitorius*, as for the experiment conducted by Joshi et al. (2016) six times more polymer solution was used.³⁶

Another core flooding experiment of Guar gum injection into a sandpack showed satisfactory results on additional oil recovery. After injection of 0.5 PV of 2000 ppm, Guar gum oil recovery increased to 15.7% from water flooding, which was 55% from the original oil in place.⁴¹

Core flooding results conducted by Said et al. (2021) showed that Xanthan gum could effectively reduce oil saturation after waterflooding. In the experiment, 3 PV of 1500 ppm Xanthan gum solution was injected into a sandstone core resulting in 13.93% of additional oil recovered Said et al. (2021). Comparing oil displacement efficiency, *C. olitorius* performed better than Xanthan gum considering the same sandstone core types and post-water flooding recovery of around 45–50%. Overall, *C. olitorius* has proved its effectiveness compared to other polymers.

4. CONCLUSIONS

In this study, a *C. olitorius* mucilage solution was prepared by drying process and then solution heating. The dried leaves were subsequently characterized. It was found that the leaves contained polysaccharides, cellulose, and hemicellulose. The

viscosity of the *C. oltorius* increases with concentrations while decreasing with temperature. The inverse proportion relationship did not follow a consistent linear trend. Despite the increase in temperature, the viscosity increased at high salinity. *C. oltorius* exhibits improved rheology under saline environments, with a 15% increase in viscosity. The properties of the natural chemical are justified by the effect of ions on bridging and restructuring the polysaccharide intramolecular and chains.

C. oltorius exhibits shear thinning behavior, indicating good match with the Ostwald–de Waele model. The flow behavior indexes decrease as the temperature increases. The salinity model revealed that as salinity increased, the flow behavior index increased, but the consistency index decreased.

The findings contribute to a better understanding of flow behavior in porous sandstone media. The chemical flood design revealed that a unit PV injected of mucilage gives an additional 10–15% recovery. Due to its superior rheology and flooding capabilities, this natural hydrocolloid has a prospective application in EOR, specifically for offshore needs.

■ AUTHOR INFORMATION

Corresponding Authors

Azza Hashim Abbas – Department of Petroleum Engineering, School of Mining and Geosciences, Nazarbayev University, Astana 010000, Kazakhstan; orcid.org/0000-0002-6090-1439; Email: azza.hashim@nu.edu.kz

Tri Thanh Pham – Department of Biology, School of Sciences and Humanities, Nazarbayev University, Astana 010000, Kazakhstan; orcid.org/0000-0003-1026-2146; Email: tri.pham@nu.edu.kz

Authors

Ghalymzhan Serikov – Department of Petroleum Engineering, School of Mining and Geosciences, Nazarbayev University, Astana 010000, Kazakhstan

Yermukhan Zhunisenov – Department of Petroleum Engineering, School of Mining and Geosciences, Nazarbayev University, Astana 010000, Kazakhstan

Neda Eghtesadi – Department of Chemical and Materials Engineering, School of Engineering and Digital Sciences, Nazarbayev University, Astana 010000, Kazakhstan

Kamel Fahmi Bou-Hamdan – Chemical & Petroleum Engineering Department, Beirut Arab University, Debbieh 1107 2809, Lebanon

Complete contact information is available at:

<https://pubs.acs.org/10.1021/acsomega.3c03834>

Author Contributions

Azza Hashim Abbas: Conceptualization, methodology, investigation, validation, and writing – original draft. **Ghalymzhan Serikov:** Experimental, investigation, and original draft. **Yermukhan Zhunisenov:** Methodology, investigation, and experimental. **Neda Eghtesadi:** Experimental and methodology. **Kamel Fahmi Bou-Hamdan:** Validation, review, and editing. **Tri Thanh Pham:** Supervision, resources, funding, review, and editing.

Funding

The authors would like to thank Nazarbayev University for supporting this research through the NU Faculty Development Competitive Research Grants Program (grant numbers: 20122022FD4137 (AHA) and 021220FD4451 (TTP)).

Notes

The authors declare no competing financial interest.

■ REFERENCES

- (1) Longinos, S. N.; Parlaktuna, M. Kinetic analysis of arginine, glycine and valine on methane (95%)–propane (5%) hydrate formation. *React. Kinet. Mech. Catal.* **2021**, *133*, 741–751.
- (2) (a) Wang, L.; Lu, X.-G.; Deng, Q.-J.; Xiao, L. EOR technology after polymer flooding and its technical and economic evaluation. *Oilfield Chem.* **2010**, *4*, 6. (b) Kemp, A.; Stephen, L. The economics of EOR schemes in the UK Continental Shelf (UKCS). In *SPE Offshore Europe Conference and Exhibition*; OnePetro, 2015.
- (3) Guo, H.; Wang, Z.; Dang, S.; Wen, R.; Lyu, X.; Liu, H.; Yang, M. What is Learned from Polymer Flooding Practices in Offshore Reservoirs?. In *Offshore Technology Conference*; OTC, 2023, p D011S014R006.
- (4) El-Masry, J. F.; Bou-Hamdan, K. F.; Abbas, A. H.; Martyushev, D. A. A Comprehensive Review on Utilizing Nanomaterials in Enhanced Oil Recovery Applications. *Energies* **2023**, *16*, 691.
- (5) (a) Trusmiyadi, Y.; Kurniawan, F.; Fitria, R.; Elias, E.; Muhyinsyah, A. Produced Water Treatment Improvements in Facing Indonesian Government Regulation on Onshore Disposed Waste Water. In *SPE Asia Pacific Oil and Gas Conference and Exhibition*; OnePetro, 2011. (b) Chai Ching Hsia, I.; M Yusof, M. F.; Hanafiah, N. Is Surfactant Environmentally Safe for Offshore Use and Discharge? An Evaluation Strategy for Chemical EOR Application in Malaysia. In *International Petroleum Technology Conference*; OnePetro, 2019. (c) Longinos, S. N.; Parlaktuna, M. Examination of behavior of lysine on methane (95%)–propane (5%) hydrate formation by the use of different impellers. *J. Pet. Explor. Prod. Technol.* **2021**, *11*, 1823–1831.
- (6) Bashir, A.; Haddad, A. S.; Rafati, R. A review of fluid displacement mechanisms in surfactant-based chemical enhanced oil recovery processes: Analyses of key influencing factors. *Petrol. Sci.* **2021**, *19*, 1211.
- (7) (a) Abbas, A. H.; Elhag, H. H.; Sulaiman, W. R. W.; Gbadamosi, A.; Pourafshary, P.; Ebrahimi, S. S.; Alqohaly, O. Y.; Agi, A. Modelling of continuous surfactant flooding application for marginal oilfields: a case study of Bentiu reservoir. *J. Pet. Explor. Prod. Technol.* **2021**, *11*, 989–1006. (b) Abbas, A. H.; Abdullah, D. S.; Jaafar, M. Z.; Wan Sulaiman, W. R.; Agi, A. Comparative numerical study for polymer alternating gas (PAG) flooding in high permeability condition. *SN Appl. Sci.* **2020**, *2*, 938. (c) Abbas, A. H.; Moslemizadeh, A.; Wan Sulaiman, W. R.; Jaafar, M. Z.; Agi, A. An insight into a di-chain surfactant adsorption onto sandstone minerals under different salinity-temperature conditions: Chemical EOR applications. *Chem. Eng. Res. Des.* **2020**, *153*, 657–665.
- (8) Derkani, M. H.; Fletcher, A. J.; Abdallah, W.; Sauerer, B.; Anderson, J.; Zhang, Z. J. Low salinity waterflooding in carbonate reservoirs: Review of interfacial mechanisms. *Colloids Interfaces* **2018**, *2*, 20.
- (9) (a) Lu, Q.; Ning, Y.; Wang, J.; Yang, X. Full Field Offshore Surfactant-Polymer Flooding in Bohai Bay China. In *SPE Asia Pacific Enhanced Oil Recovery Conference*; Society of Petroleum Engineers, 2015. (b) Zhong, H.; Zhang, W.; Fu, J.; Lu, J.; Yin, H. The Performance of Polymer Flooding in Heterogeneous Type II Reservoirs—An Experimental and Field Investigation. *Energies* **2017**, *10*, 454.
- (10) Agi, A.; Junin, R.; Gbonhinbor, J.; Onyekonwu, M. Natural polymer flow behaviour in porous media for enhanced oil recovery applications: a review. *J. Pet. Explor. Prod. Technol.* **2018**, *8*, 1349–1362.
- (11) Shi, F.; Chang, Y.; Shen, J.; Chen, G.; Xue, C. A comparative investigation of anionic polysaccharides (sulfated fucan, *t*-carrageenan, *κ*-carrageenan, and alginate) on the fabrication, stability, rheology, and digestion of multilayer emulsion. *Food Hydrocolloids* **2023**, *134*, 108081.
- (12) Saha, R.; Uppaluri, R. V. S.; Tiwari, P. Impact of Natural Surfactant (Reetha), Polymer (Xanthan Gum) and Silica Nano-

- particles to Enhance Heavy Crude Oil Recovery. *Energy Fuels* **2019**, *33*, 4225–4236.
- (13) Hill, O. F.; Ward, A. J.; Clark, C. Austin Chalk Fracturing Design Using a Crosslinked Natural Polymer as a Diverting Agent. *J. Petrol. Technol.* **1978**, *30*, 1795–1804.
- (14) Gao, C. Potential applications of Welan gum in upstream petroleum industry. *Int. J. Oil Gas Coal Eng.* **2016**, *4*, 16.
- (15) Musa, T. A.; Ibrahim, A. F.; Nasr-El-Din, H. A.; Hassan, A. New insights into guar gum as environmentally friendly polymer for enhanced oil recovery in high-salinity and high-temperature sandstone reservoirs. *J. Pet. Explor. Prod. Technol.* **2021**, *11*, 1905–1913.
- (16) Hilfer, R.; Øren, P. Dimensional analysis of pore scale and field scale immiscible displacement. *Transp. Porous Media* **1996**, *22*, 53–72.
- (17) Abbas, A. H.; Ajunwa, O. M.; Mazhit, B.; Martyshev, D. A.; Bou-Hamdan, K. F.; Alsaheb, R. A. Evaluation of OKRA (*Abelmoschus esculentus*) macromolecular solution for enhanced oil recovery in Kazakhstan carbonate reservoir. *Energies* **2022**, *15*, 6827.
- (18) Oh, S.; Kim, D.-Y. Characterization, antioxidant activities, and functional properties of mucilage extracted from *Corchorus olitorius* L. *Polymers* **2022**, *14*, 2488.
- (19) Yamazaki, E.; Murakami, K.; Kurita, O. Easy preparation of dietary fiber with the high water-holding capacity from food sources. *Plant Foods Hum. Nutr.* **2005**, *60*, 17–23.
- (20) Yamazaki, E.; Kurita, O.; Matsumura, Y. High viscosity of hydrocolloid from leaves of *Corchorus olitorius* L. *Food Hydrocolloids* **2009**, *23*, 655–660.
- (21) El-Mahdy, A. R.; El-Sebaiy, L. A. Preliminary studies on the mucilages extracted from Okra fruits, Taro tubers, Jew's mellow leaves and Fenugreek seeds. *Food Chem.* **1984**, *14*, 237–249.
- (22) McKay, S.; Oranje, P.; Helin, J.; Koek, J. H.; Kreijveld, E.; van den Abbeele, P.; Pohl, U.; Bothe, G.; Tzoumaki, M.; Aparicio-Vergara, M.; et al. Development of an affordable, sustainable and efficacious plant-based immunomodulatory food ingredient based on bell pepper or carrot RG-I pectic polysaccharides. *Nutrients* **2021**, *13*, 963.
- (23) Oyewole, O.; Oshin, T.; Atotuoma, B. *Corchorus olitorius* stem as corrosion inhibitor on mild steel in sulphuric acid. *Heliyon* **2021**, *7*, No. e06840.
- (24) Sangroniz, L.; Fernández, M.; Santamaria, A. Polymers and rheology: A tale of give and take. *Polymer* **2023**, *271*, 125811.
- (25) Abbas, A. H.; Sulaiman, W. R. W.; Jaafar, M. Z.; Agi, A. A. Laboratory Experiment Based Permeability Reduction Estimation For Enhanced Oil Recovery. *J. Eng. Sci. Technol.* **2018**, *13*, 2464–2480.
- (26) da Silva, I. L. A.; Bevitore, A. B.; Araújo Rohen, L.; Muylaert Margem, F.; de Oliveira Braga, F.; Monteiro, S. N. Characterization by Fourier transform infrared (FTIR) analysis for natural jute fiber. *Mater. Sci. Forum* **2016**, *869*, 283–287.
- (27) Jo, B.-W.; Chakraborty, S. A mild alkali treated jute fibre controlling the hydration behaviour of greener cement paste. *Sci. Rep.* **2015**, *5*, 7837.
- (28) Vârban, R.; Crişan, I.; Vârban, D.; Ona, A.; Olar, L.; Stoie, A.; Ştefan, R. Comparative FT-IR prospecting for cellulose in stems of some fiber plants: Flax, velvet leaf, hemp and jute. *Appl. Sci.* **2021**, *11*, 8570.
- (29) Ghellam, M.; Fatena, B.; Koca, İ. Physical and chemical characterization of *Corchorus olitorius* leaves dried by different drying techniques. *Discover Food* **2022**, *2*, 14.
- (30) Azubuike, C. P.; Alfa, M. A.; Oseni, B. A. Characterization and evaluation of the suspending potentials of *Corchorus olitorius* mucilage in pharmaceutical suspensions. *Trop. J. Nat. Prod. Res.* **2017**, *1*, 39–46.
- (31) Wu, Y.; Wang, K.-S.; Hu, Z.; Bai, B.; Shuler, P.; Tang, Y. A new method for fast screening of long-term thermal stability of water soluble polymers for reservoir conformance control. In *SPE Annual Technical Conference and Exhibition*; SPE, 2009, p SPE-124257-MS.
- (32) Al-Shalabi, E. W. Numerical modeling of biopolymer flooding in high-temperature high-salinity carbonate cores. In *Offshore Technology Conference Asia*; OTC, 2018, p D032S004R009.
- (33) Agi, A.; Junin, R.; Arsad, A.; Abbas, A.; Gbadamosi, A.; Azli, N. B.; Oseh, J. Synergy of the flow behaviour and disperse phase of cellulose nanoparticles in enhancing oil recovery at reservoir condition. *PLoS One* **2019**, *14*, No. e0220778.
- (34) Seright, R. S. How much polymer should be injected during a polymer flood? Review of previous and current practices. In *IOR 2017-19th European Symposium on Improved Oil Recovery*; EAGE Publications BV, 2017; Vol. 2017, pp 1–37.
- (35) (a) Agi, A.; Junin, R.; Gbonhinbor, J.; Onyekonwu, M. Natural polymer flow behaviour in porous media for enhanced oil recovery applications: a review. *J. Pet. Explor. Prod. Technol.* **2018**, *8*, 1349–1362. (b) Hatscher, S. *Schizophyllan as a biopolymer for EOR lab and field results. Winterfall*; International Energy Agency (IEA); Germany, 2016.
- (36) Joshi, S.; Al-Wahaibi, Y.; Al-Bahry, S.; Elshafie, A.; Al-Bemani, A.; Al-Hashmi, A.; Samuel, P.; Sassi, M.; Al-Farsi, H.; Al-Mandhari, M. Production and application of schizophyllan in microbial enhanced heavy oil recovery. In *SPE EOR Conference at Oil and Gas West Asia*; OnePetro, 2016.
- (37) Abbas, S.; Sanders, A. W.; Donovan, J. C. Applicability of hydroxyethylcellulose polymers for chemical EOR. In *SPE Enhanced Oil Recovery Conference*; OnePetro, 2013.
- (38) Fortenberry, R.; Hernandez, R.; Li, Z.; Delshad, M. Customizing Polymer Rheology for Application in Commercial Scale Polymer Floods. In *SPE Annual Technical Conference and Exhibition*; OnePetro, 2017.
- (39) Green, D. W.; Willhite, G. P. *Enhanced oil recovery*; Henry L. Doherty Memorial Fund of AIME, Society of Petroleum Engineers, 1998.
- (40) (a) Kong, X.; Delshad, M.; Wheeler, M. F. A Numerical Study of Benefits of Adding Polymer to WAG Processes for a Pilot Case. *SPE Reservoir Simulation Conference*; SPE, 2015. (b) Unsal, E.; Ten Berge, A.; Wever, D. Low salinity polymer flooding: Lower polymer retention and improved injectivity. *J. Petrol. Sci. Eng.* **2018**, *163*, 671–682. (c) Al-Hajri, S.; Mahmood, S. M.; Abdulelah, H.; Akbari, S. An overview on polymer retention in porous media. *Energies* **2018**, *11*, 2751.
- (41) Samanta, A.; Ojha, K.; Sarkar, A.; Mandal, A. Surfactant and surfactant-polymer flooding for enhanced oil recovery. *Adv. Petrol. Explor. Dev.* **2011**, *2*, 13–18.